

See discussions, stats, and author profiles for this publication at: <https://www.researchgate.net/publication/262266408>

Structures of Cycloserine and 2-Oxazolidinone Probed by X-ray Photoelectron Spectroscopy: Theory and Experiment

ARTICLE in THE JOURNAL OF PHYSICAL CHEMISTRY A · MAY 2014

Impact Factor: 2.69 · DOI: 10.1021/jp500308j · Source: PubMed

CITATIONS

3

READS

23

4 AUTHORS:



[Marawan Ahmed](#)

University of Alberta

22 PUBLICATIONS 44 CITATIONS

[SEE PROFILE](#)



[Feng WANG](#)

Swinburne University of Technology

208 PUBLICATIONS 1,596 CITATIONS

[SEE PROFILE](#)



[Robert G Acres](#)

Australian Synchrotron

26 PUBLICATIONS 213 CITATIONS

[SEE PROFILE](#)



[Kevin Charles Prince](#)

Sincrotrone Trieste S.C.p.A.

479 PUBLICATIONS 7,033 CITATIONS

[SEE PROFILE](#)

Structures of Cycloserine and 2-Oxazolidinone Probed by X-ray Photoelectron Spectroscopy: Theory and Experiment

Marawan Ahmed,[†] Feng Wang,[†] Robert G. Acres,[‡] and Kevin C. Prince*,^{†,‡,§}

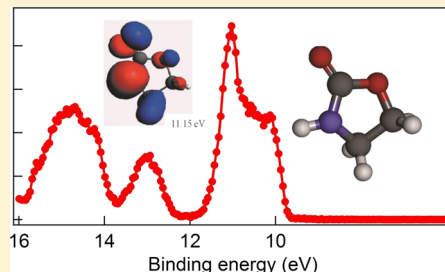
[†]eChemistry Laboratory, Department of Chemistry and Biotechnology, School of Science, Faculty of Science, Engineering and Technology, Swinburne University of Technology, Melbourne, Victoria 3122, Australia

[‡]Elettra-Sincrotrone Trieste, in Area Science Park, I-34149 Basovizza, Trieste, Italy

[§]Istituto Officina dei Materiali, Consiglio Nazionale delle Ricerche, in Area Science Park, I-34149 Basovizza, Trieste, Italy

Supporting Information

ABSTRACT: The electronic structures and properties of 2-oxazolidinone and the related compound cycloserine (CS) have been investigated using theoretical calculations and core and valence photoelectron spectroscopy. Isomerization of the central oxazolidine heterocycle and the addition of an amino group yield cycloserine. Theory correctly predicts the C, N, and O 1s core spectra, and additionally, we report theoretical natural bond orbital (NBO) charges. The valence ionization energies are also in agreement with theory and previous measurements. Although the lowest binding energy part of the spectra of the two compounds shows superficial similarities, further analysis of the charge densities of the frontier orbitals indicates substantial reorganization of the wave functions as a result of isomerization. The highest occupied molecular orbital (HOMO) of CS shows leading carbonyl π character with contributions from other heavy (non-H) atoms in the molecule, while the HOMO of 2-oxazolidinone (OX2) has leading nitrogen, carbon, and oxygen $p\pi$ characters. The present study further theoretically predicts bond resonance effects of the compounds, evidence for which is provided by our experimental measurements and published crystallographic data.



1. INTRODUCTION

In this article, we investigate theoretically and experimentally the electronic structure of two heterocyclic organic compounds of pharmacological interest, cycloserine (systematic name (4R)-4-amino-1,2-oxazolidin-3-one), denoted CS here, and 2-oxazolidinone (systematic name 1,3-oxazolidin-2-one), or OX2, Figure 1. These compounds are closely related chemically as their central rings are isomeric, and both have an oxo side group, while cycloserine has an additional amino side group.

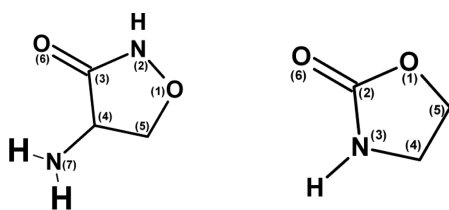


Figure 1. Schematic structure of (a) cycloserine and (b) 2-oxazolidinone, showing numbering of atoms.

Cycloserine was introduced as an antibiotic for treatment of tuberculosis and is still used as a “second line” drug for this purpose.^{1,2} Its use is restricted because of its toxic and psychotropic side effects, but it has found applications in treatment of central nervous system disorders. The other compound examined here, OX2, is also a heterocycle and its derivatives are used as drugs for treatment of Methicillin-

Resistant *Staphylococcus aureus* (MRSA), one of the greatest problems in modern hospitals.^{3–5} Other drugs are under development, based on this core chemical group.^{6,7} In the present study, we examine the free molecules and determine their basic electronic structure, unperturbed by an aqueous environment, by means of quantum chemistry calculations and photoemission experiments. This allows the unambiguous benchmarking of molecular properties and provides guidelines for further studies such as calculations of properties in an aqueous environment or intelligent/rational drug design. The present work also builds on our recent studies of some other drug-related, heterocyclic compounds, including cyclopeptides, thiazolidine carboxylic acids, and 2-azetidinone.^{8–10}

The crystal structures of the hydrochloride salt and the monohydrated zwitterion of CS have been determined previously.^{11,12} In addition, Yosa et al. have shown that the biological activities of some N-methyl-D-aspartate (NMDA) receptor ligands, including CS, can be determined by investigating the highest occupied and lowest unoccupied molecular orbitals (HOMOs and the LUMOs) of the compounds.¹³ This represents the fulfillment of a goal of an early valence band photoelectron study of OX2,¹⁴ which determined ionization potentials with a view to later correlating the data with medicinal activity. In the solid state the molecular

Received: January 10, 2014

Revised: April 25, 2014

Published: April 30, 2014



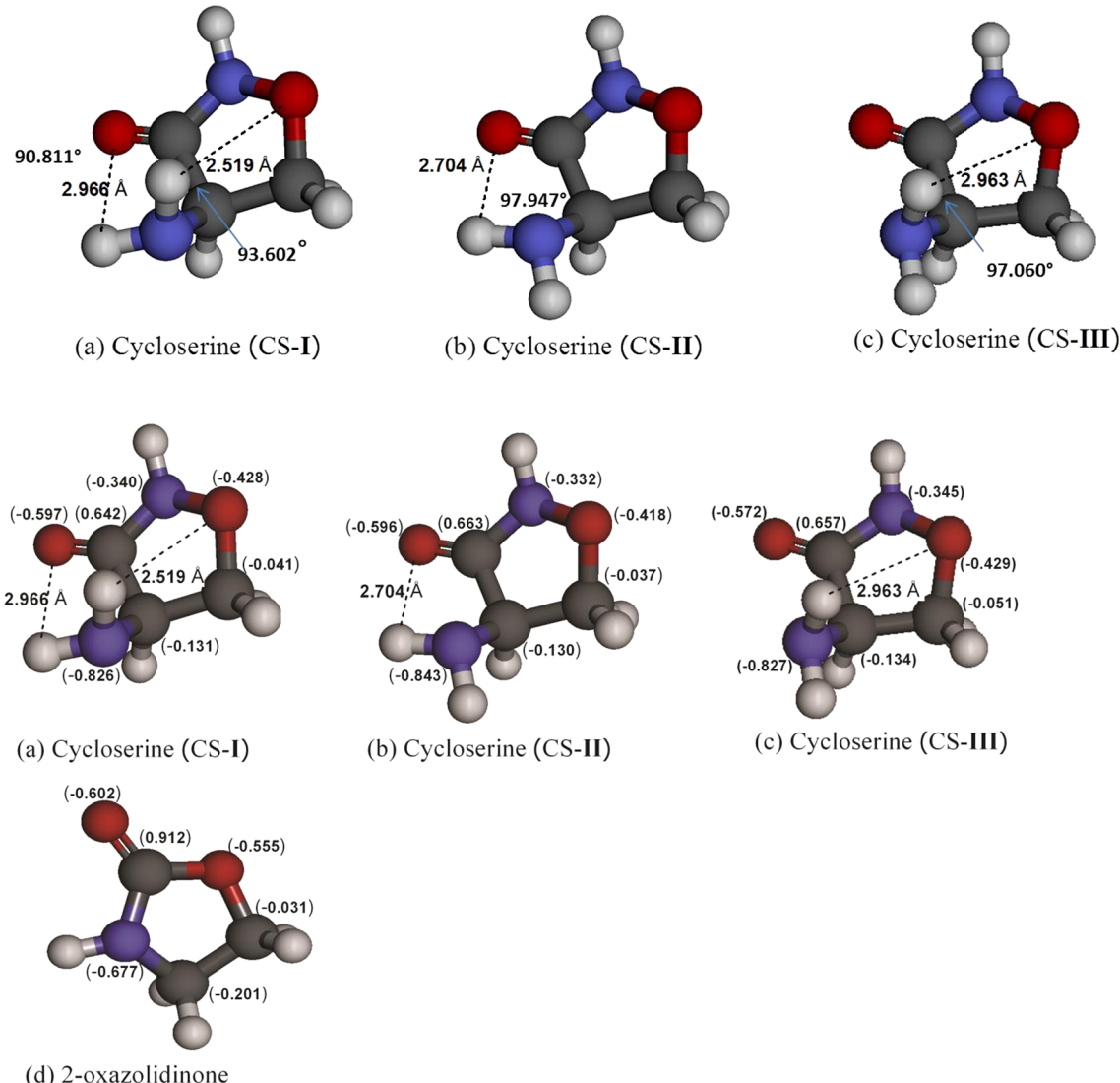


Figure 2. Three-dimensional ball and stick models of the ground state structures with potential intramolecular H-bonds distances and angles and NBO charges in parentheses of (a) cycloserine (CS-I), (b) cycloserine (CS-II), (c) cycloserine (CS-III), and (d) 2-oxazolidinone. Colors represent: red, oxygen; blue, nitrogen; dark gray, carbon; light gray, hydrogen.

structure is constrained, but in the gas phase greater conformational freedom is available. By analogy with amino acids, the primary amine group in CS may be expected to adopt various conformations, and we have investigated this possibility.

Our second compound, OX2, has been studied previously using other means,^{15,16} and its X-ray crystal structure was reported.^{17,18} The valence spectrum of OX2 has been reported previously,^{14,19} but we are not aware of any such studies of CS, and there appear to be no gas phase core ionization studies for either OX2 or CS. Andreucci et al.²⁰ measured the condensed phase valence spectra of OX2 and a number of related compounds and discussed the effect of resonance structures and delocalization of charge, a subject to which we will return later.

There are currently few computational studies of these important molecules. The current study focuses on investigating their chemical structures in the gas phase using soft X-ray photoelectron spectroscopy of the core and valence shells. In order to obtain information about how structures cause differences in functionality, the experimental measurements were used to validate our theoretical models, which are further

employed to make predictions of properties of the molecules that are not directly experimentally accessible, such as orbital character and charge distributions.

2. EXPERIMENTAL AND COMPUTATIONAL DETAILS

The measurements were performed at the gas phase photo-emission beamline of Elettra, Trieste, Italy, using apparatus and calibration methods described previously.^{21–24} The total resolution of the photons and analyzer was estimated to be 0.2, 0.32, 0.46, and 0.78 eV at photon energies of 100 (valence band), 382 (C 1s), 495 (N 1s), and 628 eV (O 1s), respectively. The compounds were supplied by Sigma-Aldrich (purity > 98%) and used without further purification. The d-enantiomer of cycloserine was used, but since the measurements and calculations were not sensitive to chiral properties, the compound is described in the following as simply cycloserine. The samples were evaporated from a non-inductively wound furnace at temperatures of 395 K for CS and 320 K for OX2. They were checked for evidence of thermal decomposition, such as spectral changes as a function of time, presence of decomposition products, which are easily identified

Table 1. Comparison of Selected Geometric Parameters of CS (Three Conformers) and OX2 with Available Theoretical and Experimental Crystal Structure Data

parameters	cycloserine				2-oxazolidinone			
	CS-I	CS-II	CS-III	exptl ^a	parameters	theory	Kaur et al. ^b	exptl ^c
R_s (Å)	7.322	7.308	7.339	7.218	R_s (Å)	7.184	7.208	7.073
$O_{(1)}-N_{(2)}$ (Å)	1.426	1.422	1.427	1.458	$O_{(1)}-C_{(2)}$ (Å)	1.371	1.377	1.356
$N_{(2)}-C_{(3)}$ (Å)	1.378	1.373	1.383	1.299	$C_{(2)}-N_{(3)}$ (Å)	1.381	1.387	1.301
$C_{(3)}-C_{(4)}$ (Å)	1.546	1.539	1.549	1.519	$N_{(3)}-C_{(4)}$ (Å)	1.455	1.470	1.466
$C_{(4)}-C_{(5)}$ (Å)	1.526	1.531	1.538	1.502	$C_{(4)}-C_{(5)}$ (Å)	1.538	1.528	1.497
$C_{(5)}-O_{(1)}$ (Å)	1.445	1.442	1.442	1.440	$C_{(5)}-O_{(1)}$ (Å)	1.440	1.446	1.453
$O_{(1)}-N_{(2)}-C_{(3)}$ (deg)	111.24	111.54	111.26	107.7	$O_{(1)}-C_{(2)}-N_{(3)}$ (deg)	108.12	108.23	110.2
$N_{(2)}-C_{(3)}-C_{(4)}$ (deg)	106.13	106.49	105.80	112.2	$C_{(2)}-N_{(3)}-C_{(4)}$ (deg)	111.09	103.95	113.3
$C_{(3)}-C_{(4)}-C_{(5)}$ (deg)	101.12	101.53	100.62	100.3	$N_{(3)}-C_{(4)}-C_{(5)}$ (deg)	99.36	98.85	100.3
$C_{(4)}-C_{(5)}-O_{(1)}$ (deg)	104.85	105.88	104.53	103.9	$C_{(4)}-C_{(5)}-O_{(1)}$ (deg)	104.49	103.95	106.0
$C_{(5)}-O_{(1)}-N_{(2)}$ (deg)	102.61	103.16	102.00	107.0	$C_{(5)}-O_{(1)}-C_{(2)}$ (deg)	109.43	108.44	108.6
ν_{\max}	37.96	34.49	40.16	29.33	ν_{\max}	26.49		
$\langle R^2 \rangle$ (au)	648.289	649.945	651.573		$\langle R^2 \rangle$ (au)	476.378		
μ (D)	1.855	2.789	3.853		μ (D)	5.519		
ZPE ^d (kJ·mol ⁻¹)	270.153	269.726	268.998		ZPE (kJ·mol ⁻¹)	229.124		
ΔE_{tot} (kJ·mol ⁻¹) ^e	0.00	5.006	13.254					
$\Delta E_{\text{tot}} + \text{ZPE}$ (kJ·mol ⁻¹)	0.00	4.582	12.010					

^aX-ray crystal structure of the monohydrated zwitterion dimer.¹² ^bB3LYP/6-31+G*.⁴⁶ ^cX-ray crystal structure.¹⁶ ^dZPE: zero point energy. ^e E_{tot} : total electron energy of the most stable conformer (CS-I) is given by $-377.934376E_h$.

in valence spectra (H_2O , CO_2 , etc.), discoloration after heating, etc. No evidence was found for decomposition of the compounds.

All geometry optimizations and calculations of natural bond orbital (NBO)²⁵ charges were performed using the density functional theory (DFT)-based B3LYP/6-31++G** model, which is incorporated in the Gaussian 09 (G09)²⁶ computational chemistry package. We also examined the conformers of CS, which are generated by rotating about the $C_{(4)}-N_{(7)}$ axis (i.e., the amino group). Three stable conformers of CS, denoted CS-I, CS-II, and CS-III and shown in Figure 2, were identified on the potential energy surface using a relaxed scan around the $C_{(3)}-C_{(4)}-N_{(7)}-H$ dihedral angle at the B3LYP/6-31G* level of theory. The B3LYP model has proven to provide reliable geometries for several biomolecules.^{27–29} The outer valence Green's function (OVGF)^{30,31} theory, which is coupled with the 6-31++G** basis set, was used to calculate valence spectra. The OVGF model, which is incorporated in the G09 computational chemistry package, accurately predicts outer-valence ionization potentials.^{8,10,32–34}

The calculations of the binding energy (ionization potential, IP) spectra were carried out using the Amsterdam Density Functional (ADF) computational chemistry program^{35–37} except for the OVGF outer-valence calculations. Core orbital calculations were performed by applying the ΔE_{KS} method³⁸ and the conventional LB94 model. The ΔE_{KS} method determines the difference in the total Kohn-Sham energies between the core-ionized cation and the neutral parent molecule using the (PW86-PW91)/et-pVQZ model, thereby taking account of the core hole relaxation effects. The vertical core ionization potentials of OX2 and CS were calculated using the LB94/et-pVQZ³⁹ model for the core-shell, and the vertical valence ionization spectra were calculated using the SAOP/et-pVQZ model.⁴⁰ Here the basis set et-pVQZ is an even-tempered polarized-valence quadruple- ζ Slater type basis set.⁴¹ The meta-Koopmans theorem^{42,43} was applied without any further modifications and scaling. The term “meta” indicates

that the Koopmans approximation is not rigorously applicable for DFT orbitals as used here, as strictly, only the negative orbital energy of the HOMO is approximately equal to the first IP. Several other software packages including Gaussview 5.0,⁴⁴ ADFVIEW,^{35–37} and Molden⁴⁵ were employed in the present study for visualization.

3. RESULTS AND DISCUSSION

3.1. Geometry and NBO Charges. The calculated geometric parameters are compared in Table 1 with available theoretical and X-ray crystallographic data.^{12,16,46} For isotropic parameters, the agreement is generally good, for example, the perimeters¹² of the rings are correctly described within 0.5 to 1.5% for the two compounds. However, anisotropic parameters such as bond angles show some discrepancies from the reported crystal structures. We attribute this to the absence of intermolecular and crystal packing forces in the gas phase, and in the case of cycloserine, to the fact that zwitterionic dimers are formed in the solid state. The experimental crystallographic data of the monohydrated form of the CS dimer are presented in Table 1.¹² Apart from this discrepancy, the overall agreement is good. A three-dimensional rendering of the structures is shown in Figure 2, with NBO charges on each atom shown in parentheses. The potential energy surface scan of CS is given in the Supporting Information (S1).

The global minimum energy conformer was calculated to be CS-I. The Gibbs free energies (ΔG) of conformers CS-II and CS-III are, respectively, 4.3 and 11.6 kJ·mol⁻¹ higher than the CS-I at the experimental temperature of 395 K. As a result, the Boltzmann populations of CS-I, CS-II, and CS-III are 77%, 21%, and 2%, respectively. The energy barriers, $\Delta TE + ZPE$, between the conformers are approximately 4.6 and 12 kJ·mol⁻¹, respectively for CS-I-CS-II and CS-I-CS-III conversions. This implies facile conversion at 395 K. The relative energies are given in Figure S2 and Table S3 of the Supporting Information.

Table 2. Comparison between Measured and Simulated Core Electron Ionization Potentials of CS (Two Conformers) and OX2 in eV

atomic site	CS				exptl	OX2				
	theory					atomic site	theory		exptl	
	CS-I	CS-II	vertical ^a	ΔE _{ks} ^b			vertical ^a	ΔE _{ks} ^b		
C ₍₃₎	292.76	293.50	292.83	293.67	293.9	C ₍₂₎	293.61	294.80	295.20	
C ₍₄₎	291.41	292.11	291.38	292.08	291.9	C ₍₄₎	291.53	292.58	292.45	
C ₍₅₎	291.74	292.64	291.68	292.58	292.3	C ₍₅₎	291.93	292.91	292.75	
N ₍₂₎	405.73	407.10	405.73	407.14	407.2	N ₍₃₎	404.34	406.20	406.2	
N ₍₇₎	403.37	405.48	403.22	405.41	405.6					
O ₍₁₎	536.63	539.54	536.53	539.47	539.85	O ₍₁₎	536.11	539.15	539.46	
O ₍₆₎	534.58	537.23	534.62	537.36	537.75	O ₍₆₎	534.27	537.26	537.55	

^aVertical IPs using the LB94/et-PVQZ model applying the meta-Koopmans theorem. ^bΔE_{ks} (PW86-PW91)/et-pVQZ.

The geometries of the three CS conformers are very similar except for the orientations of the amino group, which forms hydrogen bonds (H-bonds). For example, the bond lengths within the rings do not change appreciably, as the amino side chain orientations do not affect the ring significantly. The variation of the perimeter, R_s , of the pentagonal rings of the conformers is less than 0.02 Å, and the bond angles within the rings exhibit only small variations, as shown in Table 1. However, the dipole moments of the CS conformers do show substantial differences, as expected when a polar group adopts different conformations. The dipole moments of CS-I, CS-II, and CS-III are 1.854, 2.789, and 3.853 D. For comparison, the dipole moment of OX2 was calculated to be 5.519 D. Thus, in CS conformers, the dipole moments are significantly reduced with respect to OX2, and this is reasonable. In the conformers, the polar nitrogen and oxygen atoms are located on roughly opposite sides of the molecule, thus partly balancing their charges, while in OX2 the nitrogen and oxygen atoms are all located on one side of the molecule.

The most stable CS conformer is CS-I, which possesses two H-bonds. In this conformer, the hydrogen atoms on the N₍₇₎ amino group are rotated around the C₍₄₎–N₍₇₎ bond toward the ring, forming two H-bonds with the oxygen atoms on the ring: N₍₇₎–H_A···O₍₆₎ with a bond length of 2.966 Å, and N₍₇₎–H_B···O₍₁₎ with bond length of 2.915 Å. The CS-II and CS-III conformers are less stable, and the –NH₂ group forms only a single H-bond in each conformer. The H-bond lengths are 2.704 Å (N₍₇₎–H_B···O₍₆₎) in CS-II and 2.963 Å (N₍₇₎–H_A···O₍₁₎) in CS-III.

The geometry of OX2 is favorable for conjugation, with the carbonyl C₍₂₎ sp² hybridized and bonded to O₍₁₎ and N₍₃₎, (O₍₁₎–C₍₂₎–O₍₆₎–N₍₃₎) dihedral angle of -179.41° . The ring perimeter (R_s) of OX2 is shorter than the values for CS, theoretically by 0.138 Å and experimentally by 0.145 Å. This may be due to the existence of two resonating groups in OX2, the peptide-like (N₍₃₎C₍₂₎=O₍₆₎) group and the ester-like (O₍₁₎C₍₂₎=O₍₆₎) group, which make OX2 both a lactam (cyclic amide) and a lactone (cyclic ester). This enhanced resonance may also explain the lower theoretical puckering amplitude ν_{\max} of OX2 in the gas phase, 26.49, compared with the CS conformers, as resonance may impose a certain degree of planarity.

Figure 2 also presents the atomic site based NBO charges of the molecules at the B3LYP/6-311++G** level of theory. The atomic charge distribution in both molecules is consistent with basic electronegativity arguments, and the noncarbon heavy

atoms (N and O) possess negative NBO charges. Substitutions of nitrogen and oxygen atoms within the molecular frameworks lead to more significant charge redistributions among the molecules than conformational changes. For example, the NBO charge of the carbonyl carbon atom (C=O) in OX2 is 0.912 e, and the NBO charge for the carbonyl carbon atoms in the CS conformers is approximately 0.65 e. For the ether oxygen atom of OX2, the NBO charge is calculated to be -0.555 e but about 0.42 e for the CS conformers. For the CS conformers, the orientation of the amino group –NH₂ slightly affects the NBO charges of the atoms of the backbone frame. The changes of NBO charges on the same atoms of the molecular frame do not exceed 0.025 e among the three conformers.

It is interesting that the NBO charges on the oxygen atoms in the CS conformers are associated with their H-bond network. For example, the NBO charges of the ether oxygen, O₍₁₎, are different with and without the hydrogen bond. When H-bonded, as shown in CS-I and CS-III, the ether oxygen is more negative, -0.428 e and -0.429 e in CS-I and CS-III, respectively. However, when the ether oxygen is not H-bonded, as shown in CS-II, the NBO charge is -0.418 e. In the same way, the carbonyl oxygens are more negatively charged in CS-I and CS-II (-0.597 e and -0.596 e) due to their H-bonds, whereas the carbonyl oxygen in CS-III without an H-bond is less negative, -0.572 e.

3.2. Core Ionization Spectra. Table 2 lists the measured and calculated core ionization energies of the molecules at different levels of theory. In the table, the IPs of the two most stable CS conformers (CS-I and CS-II) are listed, but discussion will be limited to the more stable conformer CS-I. Figure 3 (upper panel) compares the measured C 1s ionization spectra of CS-I with the spectrum calculated using the ΔE_{ks} method, and they agree well. The single high energy peak is assigned to the carbonyl carbon C₍₃₎, whereas the lower energy peak and its shoulder are assigned to the C₍₅₎ and C₍₄₎ atoms with a theoretical splitting of 0.53 eV. The order of core ionization energies in CS is C₍₃₎ > C₍₅₎ > C₍₄₎, which is also predicted by the NBO charges. Theoretical IP values have the same ordering using both the LB94 and the ΔE_{ks} models.

Figure 3 (lower panel) presents the C 1s core ionization spectra of OX2. The order of the core level ionization potentials is C₍₂₎ > C₍₅₎ > C₍₄₎, which is consistent with the NBO charges, indicating that in OX2 core ionization is dominated by initial state effects. The C₍₄₎ and C₍₅₎ binding energies are similar to those in CS, consistent with the fact that the chemical environment of these two carbons is rather similar

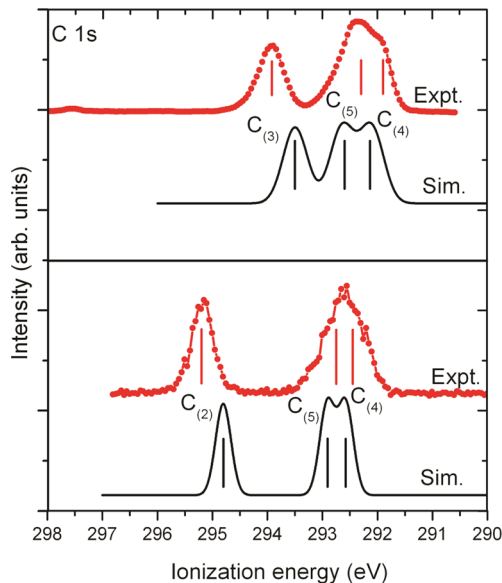


Figure 3. Experimental and simulated C 1s core ionization spectra of OX2 (lower panel, theoretical fwhm = 0.3) and CS-I (upper panel, theoretical fwhm = 0.5), using the ΔE_{ks} (PW86-PW91)/et-pVQZ level of theory.

to that in CS. The theoretical energy splitting is 0.33 eV, but the two peaks are not resolved experimentally. This value is a little lower than the energy splitting between the two lower binding energy carbons in the spectrum of CS-I ($C_{(4)}$ and $C_{(5)}$), 0.53 eV. The experimental core IP of the carbonyl carbon in OX2 is higher than that in CS-I by about 1.6 eV (theory, 1.3 eV) because this carbon is directly bonded to three electronegative atoms ($O_{(1)}$, $N_{(3)}$, and $O_{(6)}$), whereas in CS it is directly bonded to only two electronegative atoms ($N_{(2)}$ and $O_{(6)}$).

Figure 4 displays the N 1s core ionization spectra of CS-I (upper panel) and OX2 (lower panel). For CS, the peak at higher energy, IP = 407.2 eV, is assigned to the ring secondary amino nitrogen ($N_{(2)}$), while the peak at 405.6 eV is assigned to the primary amino nitrogen ($N_{(7)}$). The lower panel displays the N 1s spectra of OX2. A notable feature of the spectra is that in OX2, the N 1s IP has a value between the two N 1s core IPs of CS-I (406.2 eV), and this is directly related to the local chemical environment of each nitrogen atom. In CS, the ring nitrogen $N_{(2)}$ is bonded to a carbonyl group ($C_{(3)}=O_{(6)}$) and an oxygen atom $O_{(1)}$, while the amino nitrogen $N_{(7)}$ is not directly bonded to electronegative groups/atoms. In OX2, $N_{(3)}$ is bonded to one carbon atom and the carbonyl group ($C_{(2)}=O_{(6)}$). Thus, we expect that the binding energy of $N_{(3)}$ in OX2 is less than the binding energy of $N_{(2)}$ in CS-I. However, the question arises as to why the binding energy of $N_{(3)}$ in OX2 is higher than that of $N_{(7)}$ in CS-I since both are amino nitrogen atoms bonded to carbon atoms. We attribute the difference to resonance interaction in OX2 between $N_{(3)}$ and $O_{(6)}$, and possibly also $O_{(1)}$. In CS-I the nitrogen is a third nearest neighbor of oxygen, whereas in OX2 the two atoms are second nearest neighbors, the arrangement required for maximizing resonance interaction.⁴⁷

Figure 5 presents the measured O 1s spectra of CS-I (upper panel) and OX2 (lower panel). Theoretical spectra are shifted by +0.5 eV (CS-I) and +0.3 eV (OX2) to match the experiment. Experimentally, the higher energy oxygen peaks, IP = 539.85 eV (CS-I) and 539.46 eV (OX2) are assigned to

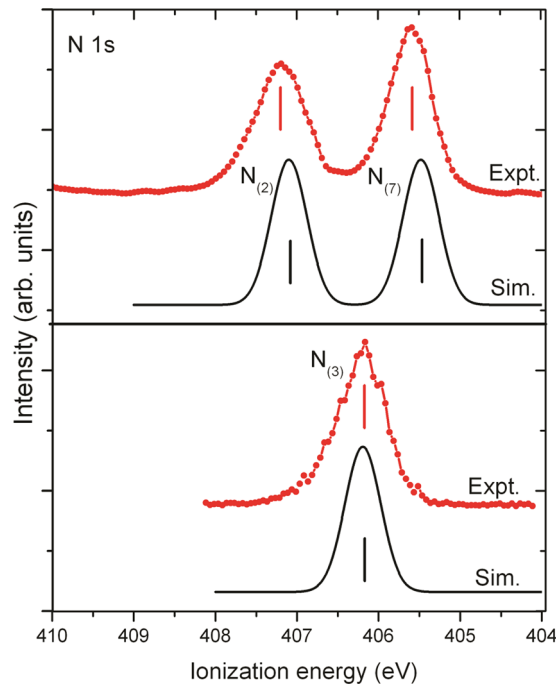


Figure 4. Experimental and simulated N 1s core ionization spectra of OX2 (lower panel) and CS-I (upper panel) using the ΔE_{ks} (PW86-PW91)/et-pVQZ level of theory and fwhm = 0.5 eV.

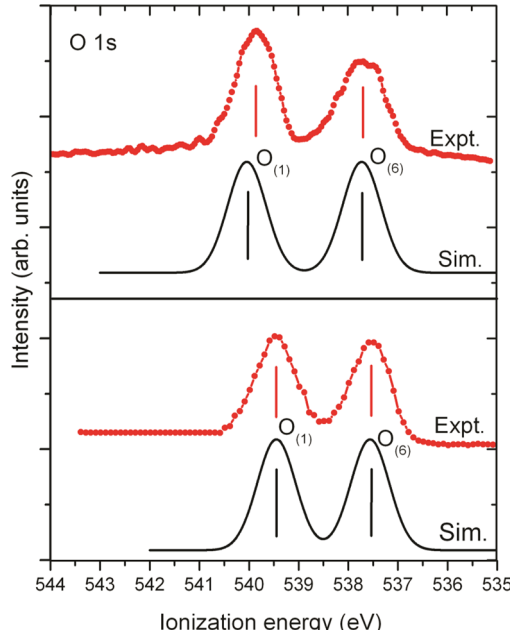


Figure 5. Experimental and simulated O 1s core ionization spectra of OX2 (lower panel, simulated spectrum is shifted by +0.3 eV to match experiment) and CS-I (upper panel, simulated spectrum is shifted by +0.5 eV to match experiment), using the ΔE_{ks} (PW86-PW91)/et-pVQZ level of theory and fwhm = 0.9 eV.

the ring oxygen $O_{(1)}$, and the lower energy peaks at 537.75 eV (CS-I) and 537.55 eV (OX2) are assigned to the carbonyl oxygen $O_{(6)}$.

Compared to OX2, the $O_{(1)}$ IP of CS-I is about 0.39 eV higher (ΔE_{ks} and experiment), which may be explained by the existence of partial double bond character in OX2 (the $O_{(1)}-C_{(2)}$ distance is 1.371 Å) due to resonance with the carbonyl

Table 3. Comparison between Measured and Simulated Valence Electron Ionization Potentials of CS (Two Conformers) and OX2 in eV

Cycloserine						2-oxazolidinone							
Orbital	CS-I		CS-II		Expt.	Orbital	SAOP ^a		OVGF ^b		Expt. ^c	Expt. ^d	Expt.
	SAOP ^a	OVGF ^b	SAOP ^a	OVGF ^b			SAOP ^a	OVGF ^b	Expt. ^c	Expt. ^d			
28a(LUMO)	5.72		5.76		9.22 (A)	24a(LUMO)	4.60						
27a(HOMO)	10.10	9.14	10.31	9.23	9.22 (A)	23a(HOMO)	11.15	10.08	10.06	10.21	10.10 (A)		
26a(HOMO-1)	10.70	9.86	10.62	10.04	9.88 (B)	22a(HOMO-1)	11.46	10.95	10.98	10.71	10.50 (B)		
25a(HOMO-2)	11.54	11.19	11.14	10.52	10.82 (C)	21a(HOMO-2)	11.94	11.21		11.07	11.04 (C)		
24a	12.82	12.41	12.84	12.35	11.94 (D)	20a	13.52	13.15	13.0	12.82	13.03 (D)		
23a	13.43	13.09	13.84	13.53	13.28 (E)	19a	14.67	14.55			14.21 (E)		
22a	14.53	14.49	14.27	14.21	14.53 (F)	18a	14.86	14.80			14.85 (F)		
21a	14.57	14.60	14.67	14.56	14.53 (F)	17a	15.02	15.01					
20a	15.13	15.02	15.13	15.01	-	16a	15.18	15.21					
19a	15.55	15.46	15.24	15.01	-	15a	16.43	16.48			16.36 (G)		
18a	15.72	15.79	15.69	15.84	15.74 (G)	14a	17.51	17.79	17.51	17.79	17.65 (H)		
17a	16.34	16.58	16.74	17.06	-	13a	17.68	17.92					
16a	17.40	17.65	17.13	17.37	-	12a	19.77				19.92 (I)		
15a	17.61	17.81	17.67	17.77	17.98 (H)	11a	20.82				21.5 (J)		
14a	19.68		19.56		19.61 (I)	10a	23.64				24.5 (K)		
13a	20.34		20.41		20.76 (J)	9a	27.95				29.1 (L)		
12a	23.44		23.45		24.18 (K)	8a	30.34				31.5 (M)		
11a	26.13		26.16		-	7a	32.61				34 (N)		
10a	27.07		27.00		27.6 (L)								
9a	30.72		30.80		-								
8a	32.52		32.51		33.2 (M)								
HOMO-LUMO gap		4.39	4.55		HOMO-LUMO gap 6.55								

^aSAOP/et-pVQZ. ^bOVGF/6-311++G**. ^cAndreocci et al.¹⁹ ^dGerson et al.¹⁴

group, which is directly attached to this oxygen in OX2 but not in CS.

3.3. Valence Ionization Spectra. The calculated and measured valence band energies of both compounds are displayed in Table 3, and the data are plotted in Figures 6 and 7. For CS, the theoretical curve is the Boltzmann weighted sum of the two lowest energy conformers, CS-I and CS-II. The spectroscopic pole strengths calculated using the OVGF model are all between 0.89 and 0.91, indicating that the single particle approximation used in the models is valid.

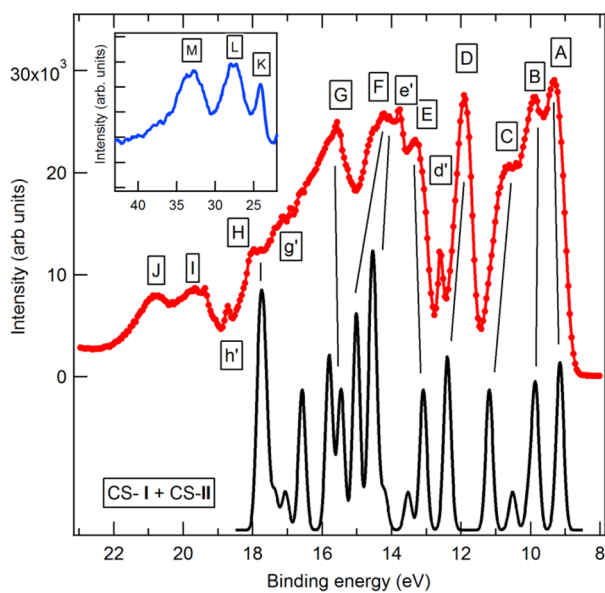


Figure 6. Experimental and OVGF/6-311++G** simulated valence band photoelectron spectra of cycloserine. Inset: inner valence band. Photon energy: 100 eV. The simulated spectrum of conformers is weighted by their calculated Boltzmann factors at the experimental temperature. The simulated spectrum is broadened by fwhm = 0.25 eV.

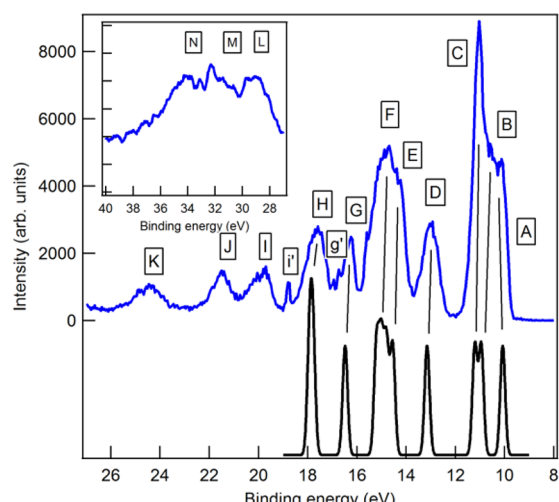


Figure 7. Experimental and OVGF/6-311++G** simulated valence band photoelectron spectra of oxazolidinone. Inset: inner valence band. Photon energy: 100 eV. The simulated spectrum is broadened by fwhm = 0.25 eV.

The features of the valence spectrum of cycloserine (Figure 6) are labeled from A to M. A number of weak features appear due to the residual gas in the experimental chamber, which consists mostly of water (feature d'), carbon dioxide (e'), and nitrogen (g' and h'), and are easily identified by their very narrow line widths. In Table 3, the vertical ionization energies are compared with values calculated using the SAOP and OVGF methods. The first seven valence states observed experimentally can be unambiguously assigned to ionization of molecular orbitals 27a to 21a, as calculated by OVGF. No clear features appear, which can be associated with orbitals 20a, 19a, 17a, and 16a, but in the experimental spectrum, there is clearly intensity in the regions where these ionic states are expected. We conclude that these particular states are either broadened so much that they cannot be distinguished or that they overlap two-hole, one-particle states, which obscure them, or that both

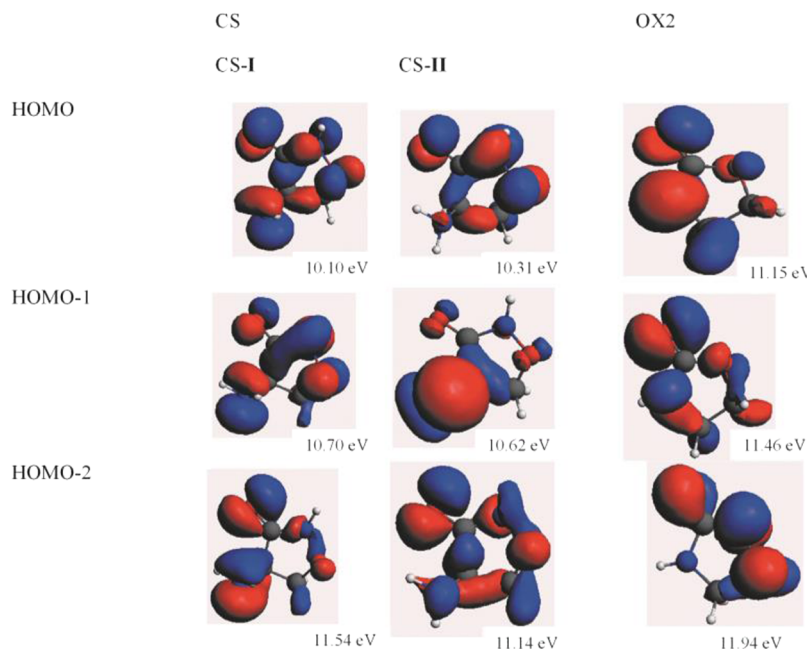


Figure 8. Electronic charge distribution of the frontier orbitals of CS and OX2, SAOP/et-pVQZ.

effects are present. Valence states 18a and 15a are clearly identified as well as those mentioned above.

The theoretical spectrum takes into account two conformers weighted according to the calculated populations, but cross sections have not been calculated. Thus, quantitative agreement with the intensities is not expected, and we focus on the energies of the features. There is no unambiguous evidence for the presence of two conformers, and the spectrum can be explained assuming a single conformer CS-I. Theory predicts that the HOMO-2 of the conformers CS-I and CS-II should have significantly different binding energies, giving rise to four features in the 9 to 12 eV binding energy range. We also measured spectra at various photon energies from 40 to 100 eV (not shown), with the goal of observing possible effects due to differences in cross-section in the region of the HOMO-2 peak. However, all spectra were adequately fitted by assuming three peaks, so no additional evidence of conformers was found. We conclude that experimental techniques that are sensitive to rotational conformers are needed for conclusive information regarding the existence of the CS-II conformer.

For the inner valence region at higher binding energies, the OVGF calculations do not make predictions, and we turn to the SAOP calculations. This method allows us to assign the single-hole states in this region, although there are many two-hole, one-particle states as well, which tend to add a continuum background to the spectrum and cause energy shifts due to configuration interaction. The features I to M can be assigned to valence singly ionized states. No clear features were identified, which can be associated with the valence orbitals 11a and 9a, and again we ascribe this to effects of broadening or overlap with excited final states.

Considering the first 9 predicted and observed outer valence ionic states, the OVGF formalism predicts the energies with a mean deviation from experiment of 0.22 eV. The SAOP calculations fare worse, with a mean deviation of 0.49 eV from the experimental values, and the greatest discrepancies here are for the HOMO and HOMO-3 molecular orbitals. At higher

binding energies, the agreement improves and provides assignments for some of the inner valence features, as noted.

For oxazolidinone, Figure 7, theory predicts that the first band consists of three ionic states, A (23a), B (22a), and C (21a), and this explains its unusual shape, in which two peaks are clearly distinguished (A and C), while the remaining peak (B) appears to be a shoulder, but might have been due to vibrational structure. In a previous study with He I radiation,¹⁹ this region of the spectrum appeared to consist of only two peaks. The fitted widths of these three states vary from 230 to 360 meV or 113 to 300 meV after subtracting the resolution in quadrature. These very narrow line widths, of the order of a single vibrational quantum, suggest that the Franck-Condon envelopes of these states contain very few vibrational states. From this we conclude that the ground and excited state potential energy curves and equilibrium bond distances are very similar and that these orbitals have mostly nonbonding character.

The next state D is assigned to ionization of orbital 20a. Features E and F are asymmetric and can be fitted with only two peaks. Theory indicates that four ionic states contribute to this structure: ionization of orbitals 19a to 16a. The intensity of features E and F, much higher than the preceding or following peaks, is qualitatively consistent with the assignment to ionization of more than two orbitals. Similarly peak G is assigned to a single state, while peak H is due to two states. The higher binding energy peaks are not calculated by the OVGF method, which considers only the outer valence, so they are assigned as shown in Table 3 on the basis of the SAOP calculations. In this energy range, there are many two-hole, single-particle states, so the calculations provide only the main character of the stronger spectral features.

The average difference between the calculated OVGF ionization potentials and the experimental values is 0.2 eV. For the SAOP calculations, the difference is larger, 0.40 eV if we include only the peaks calculated using OVGF, or 0.59 eV if all calculated orbitals are included. Also, the discrepancies are large for the HOMO and HOMO-1 (SAOP orbitals), where

the ionization potentials are overestimated, but the agreement improves for intermediate orbitals. For inner valence orbitals, the discrepancy is again large, but the sign of the difference changes and the SAOP calculations underestimate the energies.

The orbital character of the valence states can be determined by mapping the ground state charge density of the orbitals, Figure 8. The HOMO of both conformers of CS consists of an extended molecular orbital with π character involving the C=O bond but extending over all heavy atoms of the heterocycle. The HOMO of OX2 is also based on atomic orbitals of N₍₃₎ p π , O₍₆₎ p π , and C₍₄₎ p π character but is more heavily localized on the N₍₃₎—C₍₄₎ bond than the other heavy atoms. The HOMO-1 orbitals of the two conformers of CS show many more significant differences than the HOMO or HOMO-2 orbitals. In conformer I the orbital is delocalized over most of the molecule, but in conformer II, it is localized on the primary amino group with strong N₍₇₎ p π character. The HOMO-1 of OX2 does not appear to be similar in character to the HOMO-1 orbitals of the CS conformers.

The HOMO-2 of CS-I is largely localized on O₍₆₎—C₍₄₎—N₍₇₎, while that of conformer II is delocalized over the molecule. The corresponding orbital of OX2 is composed of p type orbitals localized on O₍₁₎—C₍₅₎—C₍₃₎. Considering CS as an isomerized derivative of OX2, the orbitals appear to undergo two changes. First there is a change in the energy ordering, as the HOMO-2 of OX2 most closely resembles the HOMO of conformer II of CS. Similarly the HOMO-1 of OX2 shows some resemblance to the HOMO-3 of conformer I. Second there is a stronger effect of mixing and rearrangement of the orbital character so that the orbitals of CS become distinct from those of OX2.

As mentioned above, we have evidence for resonance phenomena from the geometrical structure and we therefore expect that some molecular orbitals will have π character and be localized on the atoms displaying resonance. We examined the character of the valence orbitals and we find the orbitals shown in Figure 9, orbital 18a (HOMO-9) of CS-I and orbital 18a

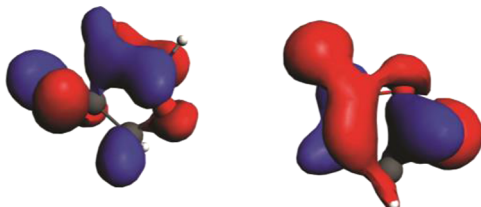


Figure 9. Left: orbital 18a (HOMO-9) of CS-I. Right: orbital 18a (HOMO-5) in OX2, SAOP/et-pVQZ.

(HOMO-5) of OX2, have the expected charge distribution. In CS, the molecular orbital is made up of atomic p_z contributions from O₍₁₎, N₍₂₎, the carbonyl group, and N₍₇₎, while in OX2 the corresponding orbitals of the carbonyl group and N₍₃₎ are mixed, with a contribution from C₍₅₎. Thus, the valence molecular orbital charge distribution, the bonding geometry, and the core level spectra are consistent with the existence of resonance effects in both molecules.

Interestingly, the effect of conformerism, which involves simple twisting of covalent bonds and formation or breaking of hydrogen bonds, has quite a strong effect on the character of the molecular orbitals. Presumably this is primarily because of changes in the extent of spatial overlap of the relevant atomic orbitals.

4. CONCLUSIONS

In the present study, the core and valence soft X-ray photoelectron spectra of cycloserine and 2-oxazolidinone have been determined and assigned applying high quality quantum mechanical calculations. The character of the frontier valence orbitals has been assigned, and the core level spectra related to the electronic structure. Although theory predicted that two conformers of cycloserine were populated, we were unable to find unambiguous experimental evidence of this. On the other hand, theoretical analysis predicted resonance effects in the valence bonding and identified the molecular orbitals involved. Core level spectra and published bond lengths support this interpretation, leading to a consistent picture of the electronic structure.

■ ASSOCIATED CONTENT

S Supporting Information

CS potential energy surface scan together with the relative energy and populations of the most stable CS conformers. This material is available free of charge via the Internet at <http://pubs.acs.org>.

■ AUTHOR INFORMATION

Corresponding Author

*(K.C.P.) Phone: +39 0403758584. Fax: +39 0403758565. E-mail: kevin.prince@elettra.trieste.it.

Notes

The authors declare no competing financial interest.

■ ACKNOWLEDGMENTS

The authors wish to thank Professor D. P. Chong for his assistance in the Δ DFT calculations. M.A. acknowledges the Swinburne University Postgraduate Research Award (SUPRA). F.W. acknowledges the Australian Synchrotron for international synchrotron access program support; she also thanks the Victorian Partnership for Advanced Computing (VPAC) and Swinburne University supercomputing (Green/gSTAR) for support on the computing facilities. The National Computational Infrastructure (NCI) at the Australian National University and the Victorian Life Sciences Computation Initiative (VLSCI) on its Peak Computing Facility at the University of Melbourne (an initiative of the Victorian Government, Australia) under the National Computational Merit Allocation Scheme (NCMAS) are acknowledged. We thank our colleagues at Elettra-Sincrotrone Trieste for providing high quality synchrotron light.

■ REFERENCES

- Grzembska, M.; Mihaescu, T.; Clancy, L.; Casali, L. Tuberculosis Management in Europe. *Eur. Respir. J.* **1999**, *14*, 978–992.
- Mdluli, K.; Spigelman, M. Novel Targets for Tuberculosis Drug Discovery. *Curr. Opin. Pharmacol.* **2006**, *6*, 459–467.
- Tsiodras, S.; Gold, H. S.; Sakoulas, G.; Eliopoulos, G. M.; Wennersten, C.; Venkataraman, L.; Moellering, R. C.; Ferraro, M. J. Linezolid Resistance in a Clinical Isolate of *Staphylococcus aureus*. *Lancet* **2001**, *358*, 207–208.
- Dennis, L. S.; Daniel, H.; Harry, L.; John, L. H.; Donald, H. B.; Barry, H. Linezolid Versus Vancomycin for the Treatment of Methicillin-Resistant *Staphylococcus aureus* Infections. *Clin. Infect. Dis.* **2002**, *34*, 1481–1490.
- Li, Z.; Willke, R. J.; Pinto, L. A.; Rittenhouse, B. E.; Rybak, M. J.; Pleil, A. M.; Crouch, C. W.; Hafkin, B.; Glick, H. A. Comparison of Length of Hospital Stay for Patients with Known or Suspected

- Methicillin-Resistant *Staphylococcus* Species Infections Treated with Linezolid or Vancomycin: A Randomized, Multicenter Trial. *Pharmacotherapy* **2001**, *21*, 263–274.
- (6) Lohray, B. B.; Baskaran, S.; Srinivasa Rao, B.; Yadi Reddy, B.; Nageswara Rao, I. A Short Synthesis of Oxazolidinone Derivatives Linezolid and Eperezolid: A New Class of Antibacterials. *Tetrahedron Lett.* **1999**, *40*, 4855–4856.
- (7) Hutchinson, D. K. Oxazolidinone Antibacterial Agents: A Critical Review. *Curr. Top. Med. Chem.* **2003**, *3*, 1021–1042.
- (8) Arachchilage, A. P. W.; Wang, F.; Feyer, V.; Plekan, O.; Prince, K. C. Correlation of Electronic Structures of Three Cyclic Dipeptides with Their Photoemission Spectra. *J. Chem. Phys.* **2010**, *133*, 174319–174329.
- (9) Arachchilage, A. P. W.; Wang, F.; Feyer, V.; Plekan, O.; Prince, K. C. Photoelectron Spectra and Structures of Three Cyclic Dipeptides: PhePhe, TyrPro, and HisGly. *J. Chem. Phys.* **2012**, *136*, 124301–124309.
- (10) Ahmed, M.; Ganesan, A.; Wang, F.; Feyer, V.; Plekan, O.; Prince, K. C. Photoelectron Spectra of Some Antibiotic Building Blocks: 2-Azetidinone and Thiazolidine-Carboxylic Acid. *J. Phys. Chem. A* **2012**, *116*, 8653–8660.
- (11) Turley, J. W.; Pepinsky, R. Further Refinement of the Crystal Structure of Cycloserine Hydrochloride. *Acta Crystallogr.* **1957**, *10*, 480–481.
- (12) Lee, H.-H.; Takeuchi, N.; Senda, H.; Kuwae, A.; Hanai, K. Molecular Structure and Dimerization of D-Cycloserine in the Solid State. *Spectrosc. Lett.* **1998**, *31*, 1217–1231.
- (13) Yosa, J.; Blanco, M.; Acevedo, O.; Lareo, L. R. Molecular Orbital Differentiation of Agonist and Antagonist Activity in the GlycineB-iGluR-NMDA Receptor. *Eur. J. Med. Chem.* **2009**, *44*, 2960–2966.
- (14) Gerson, S. H.; Worley, S. D.; Bodor, N.; Kaminski, J. J.; Flechtner, T. W. The Photoelectron Spectra of Some Heterocyclic Compounds Which Contain N, O, Cl and Br. *J. Electron Spectrosc. Relat. Phenom.* **1978**, *13*, 421–434.
- (15) Okumoto, S.; Yamabe, S. A Computational Study of Base-Catalyzed Reactions between Isocyanates and Epoxides Affording 2-Oxazolidones and Isocyanurates. *J. Comput. Chem.* **2001**, *22*, 316–326.
- (16) Pankratov, V. A.; Frenkel, T. M.; Fainleib, A. M. 2-Oxazolidinones. *Russ. Chem. Rev.* **1983**, *52*, 576–593.
- (17) Wouters, J.; Ooms, F.; Durant, F. 2-Oxazolidinone. *Acta Crystallogr., Sect. C: Cryst. Struct. Commun.* **1997**, *53*, 895–897.
- (18) Flakus, H. T.; Michta, A. Polarization IR Spectra of the Hydrogen Bond in 2-Oxazolidone Crystals: Isotopic Dilution Effects in the Crystalline Spectra. *Vib. Spectrosc.* **2003**, *33*, 177–187.
- (19) Andreucci, M. V.; Devillanova, F. A.; Furlani, C.; Mattogno, G.; Verani, G.; Zanoni, R. Structural Characterization of Some Substituted Azolidine Molecules: UPS Photoelectron Spectroscopic Studies. *J. Mol. Struct.* **1980**, *69*, 151–163.
- (20) Andreucci, M. V.; Bossa, M.; Devillanova, F. A.; Furlani, C.; Mattogno, G.; Verani, G.; Zanoni, R. Structural Characterization of Some Substituted Azolidine Molecules; X-Ray Photoelectron Spectroscopic Results. *J. Mol. Struct.* **1981**, *71*, 227–236.
- (21) Plekan, O.; Feyer, V.; Richter, R.; Coreno, M.; de Simone, M.; Prince, K. C.; Carravetta, V. Photoemission and the Shape of Amino Acids. *Chem. Phys. Lett.* **2007**, *442*, 429–433.
- (22) Plekan, O.; Feyer, V.; Richter, R.; Coreno, M.; de Simone, M.; Prince, K. C.; Carravetta, V. Investigation of the Amino Acids Glycine, Proline, and Methionine by Photoemission Spectroscopy. *J. Phys. Chem. A* **2007**, *111*, 10998–11005.
- (23) Plekan, O.; Feyer, V.; Richter, R.; Coreno, M.; de Simone, M.; Prince, K. C.; Carravetta, V. An X-Ray Absorption Study of Glycine, Methionine and Proline. *J. Electron Spectrosc. Relat. Phenom.* **2007**, *155*, 47–53.
- (24) Feyer, V.; Plekan, O.; Richter, R.; Coreno, M.; de Simone, M.; Prince, K. C.; Trofimov, A. B.; Zaytseva, I. L.; Schirmer, J. Tautomerism in Cytosine and Uracil: A Theoretical and Experimental X-Ray Absorption and Resonant Auger Study. *J. Phys. Chem. A* **2010**, *114*, 10270–10276.
- (25) Weinhold, F.; Landis, C. R. Natural Bond Orbitals and Extensions of Localized Bonding Concepts. *Chem. Educ. Res. Pract.* **2001**, *2*, 91–104.
- (26) Frisch, M. J.; Trucks, G. W.; Schlegel, H. B.; Scuseria, G. E.; Robb, M. A.; Cheeseman, J. R.; Scalmani, G.; Barone, V.; Mennucci, B.; Petersson, G. A. et al. *Gaussian 09*; Gaussian, Inc.: Wallingford, CT, 2009.
- (27) Falzon, C. T.; Wang, F. Understanding Glycine Conformation through Molecular Orbitals. *J. Chem. Phys.* **2005**, *123*, 214307–214312.
- (28) Falzon, C. T.; Wang, F.; Pang, W. Orbital Signatures of Methyl in L-Alanine. *J. Phys. Chem. B* **2006**, *110*, 9713–9719.
- (29) Ganesan, A.; Wang, F. Intramolecular Interactions of L-Phenylalanine Revealed by Inner Shell Chemical Shift. *J. Chem. Phys.* **2009**, *131*, 044321–044329.
- (30) Schirmer, J.; Cederbaum, L. S.; Walter, O. New Approach to the One-Particle Green's Function for Finite Fermi Systems. *Phys. Rev. A* **1983**, *28*, 1237–1259.
- (31) Danovich, D. Green's Function Methods for Calculating Ionization Potentials, Electron Affinities, and Excitation Energies. *WIREs Comput. Mol. Sci.* **2011**, *1*, 377–387.
- (32) Ganesan, A.; Wang, F.; Brunger, M.; Prince, K. Effects of Alkyl Side Chains on Properties of Aliphatic Amino Acids Probed Using Quantum Chemical Calculations. *J. Synchrotron Radiat.* **2011**, *18*, 733–742.
- (33) Selvam, L.; Vasilyev, V.; Wang, F. Methylation of Zebularine: A Quantum Mechanical Study Incorporating Interactive 3D PDF Graphs. *J. Phys. Chem. B* **2009**, *113*, 11496–11504.
- (34) Chen, F.; Wang, F. Electronic Structure of the Azide Group in 3'-Azido-3'-Deoxythymidine (AZT) Compared to Small Azide Compounds. *Molecules* **2009**, *14*, 2656–2668.
- (35) te Velde, G.; Bickelhaupt, F. M.; Baerends, E. J.; Fonseca Guerra, C.; van Gisbergen, S. J. A.; Snijders, J. G.; Ziegler, T. Chemistry with ADF. *J. Comput. Chem.* **2001**, *22*, 931–967.
- (36) Fonseca Guerra, C.; Snijders, J. G.; te Velde, G.; Baerends, E. J. Towards an Order-N DFT Method. *Theor. Chem. Acc.* **1998**, *99*, 391–403.
- (37) ADF2010; Vrije University: Amsterdam, The Netherlands.
- (38) Takahata, Y.; Wulfman, C. E.; Chong, D. P. Accurate Calculation of N1s and C1s Core Electron Binding Energies of Substituted Pyridines. Correlation with Basicity and with Hammett Substituent Constants. *J. Mol. Struct.* **2008**, *863*, 33–38.
- (39) van Leeuwen, R.; Baerends, E. J. Exchange-Correlation Potential with Correct Asymptotic Behavior. *Phys. Rev. A* **1994**, *49*, 2421–2431.
- (40) Schipper, P. R. T.; Gritsenko, O. V.; van Gisbergen, S. J. A.; Baerends, E. J. Molecular Calculations of Excitation Energies and (Hyper)Polarizabilities with a Statistical Average of Orbital Model Exchange-Correlation Potentials. *J. Chem. Phys.* **2000**, *112*, 1344–1352.
- (41) Chong, D. P.; Van Lenthe, E.; Van Gisbergen, S.; Baerends, E. J. Even-Tempered Slater-Type Orbitals Revisited: From Hydrogen to Krypton. *J. Comput. Chem.* **2004**, *25*, 1030–1036.
- (42) Koopmans, T. Über Die Zuordnung Von Wellenfunktionen Und Eigenwerten Zu Den Einzelnen Elektronen Eines Atoms. *Physica* **1** *1933*, *1*, 104–113.
- (43) Janak, J. F. Proof That $\partial E/\partial N_i = E$ in Density-Functional Theory. *Phys. Rev. B* **1978**, *18*, 7165.
- (44) Dennington, R.; Keith, T.; Millam, J. *Gaussview*, version 5; Semichem Inc.: Shawnee Mission, KS, 2009.
- (45) Schaftenaar, G.; Noordik, J. H. Molden: A Pre- and Post-Processing Program for Molecular and Electronic Structures. *J. Comput.-Aided Mol. Des.* **2000**, *14*, 123–134.
- (46) Kaur, D.; Sharma, R. Factors Affecting Relative Stabilities and Proton Affinities of Oxazolidinone and Its N,C5-Formyl Derivatives. *Struct. Chem.* **2012**, *23*, 905–919.
- (47) Bolognesi, P.; Mattioli, G.; O'Keeffe, P.; Feyer, V.; Plekan, O.; Ovcharenko, Y.; Prince, K. C.; Coreno, M.; Amore Bonapasta, A.; Avaldi, L. Investigation of Halogenated Pyrimidines by X-Ray

Photoemission Spectroscopy and Theoretical DFT Methods. *J. Phys. Chem. A* **2009**, *113*, 13593–13600.